CORRIGENDUM TO:

Twin-Rudder-System Configurations' Impact on Ferry Ships' Course-Keeping Ability under Windy Conditions

Andi Haris Muhammad[1i], Daeng Paroka[2], Sabaruddin Rahman[2], Mohammad Rizal Firmansyah[3]

[1]*Departement of Marine Engineering, Faculty of Engineering, Hasanuddin University, Gowa 92171, Indonesia*
[2]*Departement of Ocean Engineering, Faculty of Engineering, Hasanuddin University, Gowa 92171, Indonesia*
[3]*Departement of Naval Architecture, Faculty of Engineering, Hasanuddin University, Gowa 92171, Indonesia*

In Equations 1 and 10 on pages 434 and 436, typed as:

$$m(\dot{u} - rv) = X_H + X_P + X_R + X_W$$
$$m(\dot{v} - ru) = Y_H + Y_P + Y_R + Y_W \tag{1}$$
$$I_{ZZ}\dot{\psi} = N_H + N_P + N_R + N_W$$

$$\delta = K_p(e) + K_d(\dot{e}) + K_i \int_0^T e(t)dt \text{ and } e = (\psi_T - \psi_P) \tag{10}$$

The equations 1 and 10 should be written as follow:

$$m(\dot{u} - rv) = X_H + X_P + X_R + X_W$$
$$m(\dot{v} - ru) = Y_H + Y_P + Y_R + Y_W \tag{1}$$
$$I_{ZZ}\dot{\psi} = N_H + N_P + N_R + N_W$$

$$\delta = K_P(e) + K_d(\dot{e}) + K_i \int_0^T e(t)dt \text{ and } e = (\psi_T - \psi_P) \tag{10}$$

Twin-Rudder-System Configurations' Impact on Ferry Ships' Course-Keeping Ability under Windy Conditions

Andi Haris Muhammad[1*], Daeng Paroka[2], Sabaruddin Rahman[2], Mohammad Rizal Firmansyah[3]

[1]*Departement of Marine Engineering, Faculty of Engineering, Hasanuddin University, Gowa 92171, Indonesia*
[2]*Departement of Ocean Engineering, Faculty of Engineering, Hasanuddin University, Gowa 92171, Indonesia*
[3]*Departement of Naval Architecture, Faculty of Engineering, Hasanuddin University, Gowa 92171, Indonesia*

Abstract. Ship course-keeping plays a vital role in navigation safety, especially when a ship is operating under windy conditions. A method to control ship movements through rudder-system configuration is necessary to stabilize a ship's course. This paper describes the twin-rudder-system configuration design's impact on a ship's course-keeping ability under windy conditions. A time-domain simulation using the MATLAB-Simulink program was developed for this purpose. A proportional integral derivative (PID) controller was used to adjust the ship's heading angle according to the desired path. Several parameters—such as relative wind velocity and directions—were accounted for in the simulation. The result shows that, at a wind direction of 88°, the ship's course-keeping speed decreased; however, increasing wind velocity caused a large deviation in the ship's heading angle. Meanwhile, the ship's course-keeping speed increased with rising windspeed directions of 219°. The ship's course-keeping time, at around 219° under the simulation's wind direction, was 11.84% lower than during a previous sea-trial. A possible reason for this difference is that the simulation excluded waves and currents.

Keywords: Course-keeping; Proportional integral derivative controller; Ship-tracking; Simulation

1. Introduction

Course-keeping quality is significant in ship navigation due to time-saving and reduced fuel consumption (Prpic-Orsic et al., 2016). To achieve quality ship course-keeping and generate accurate heading angles, a controller that considers ship hydrodynamics—including both internal and external disturbance parameters—should be installed (Lee et al, 2009). Keeping a ferry ship on course differs from sea-going ships due to navigation environments and ship particulars (Prpic-Orsic et al., 2016). The navigation environment's complexity, and especially wind-load forces and moment, makes ferry ships with large superstructures more susceptible to marine accidents (Fujiwara and Ueno, 2006). Many studies have related wind effects to ship maneuvering; wind's load-force and moment have significantly affected transversal and lateral projections of windage areas due to ships' large superstructures, as well as wind velocities and directions relative to ships (Fujiwara and Ueno, 2006). Paroka et al. (2016) simulated wind's effect on ferry ships' maneuvering,

explaining that ship-speed changes caused by wind highly depend on wind velocity and direction. When the wind blows from the bow direction and passes to the ship's starboard (0 to 100°), ship speed tends to decrease. The corresponding decrease in ship speed is insignificant when the wind blows from a starboard direction and passes to the ship's stern (100 to 180°). Meanwhile, when the wind blows from the side of a ship (20 to 140°), it tends to change the ship's direction. A ship's directional deviations due to wind vary by ship type, and a steering response is required. Ohtsu et al. (1996) reported that a wind blowing from starboard-bow quarters (45°) made a ship's steering becomes less sensitive, but steering became more sensitive when the wind came from the port-stern quarters (135°). Increasing a ship's speed as wind directions change is crucial (Ohtsu et al., 1996; Paroka et al., 2016). The information informing this behavior is essential to improve ships' course-keeping quality—especially when ships must take appropriate action to handle wind disturbances. The improving quality of a ship's course-keeping ability in windy conditions is strongly influenced by steering responses to wind-blowing loads through an appropriately configured rudder system design (Hasegawa et al., 2006). Steering control plays an essential role in responding to external forces to a ship's yaw motion stability and course-keeping ability during maneuvers (Paroka, 2020).

Many efforts to improve ships' maneuvering have been conducted using twin-rudder ship controllers. Yoshimura and Sakurai (1989) investigated the effect of a ship-fitted, twin-rudder, twin-propeller configuration on ships' maneuvering. They found that a twin-rudder, twin-propeller configuration's hydrodynamic characteristics did not differ significantly from the corresponding characteristics of a single-propeller, single-rudder ship. Khanfir et al. (2008) proposed predicting a mathematical model coefficient on ships' maneuvering when fitted with a twin-propeller, twin-rudder configuration. Furthermore, Khanfir et al. (2011) conducted captive model tests and free-running tests with a single-propeller, twin-rudder ship and a twin-propeller, twin-rudder ship. These tests aimed to evaluate drift angles' effect on rudder forces and the peculiar phenomena concerning a normal rudder force for twin-rudder ships.

Other parameters that affect ships' maneuvering performance include the distance of spacing between single rudders in twin-rudder ships. Gim (2013) conducted a twin-rudder performance test in a circulating water channel using particle image velocimetry (PIV). He set the distance between two single rudders to 0.5–1.0 times the chord length of the rudder. He found that this spacing distance between rudders in twin-rudder configurations was also affected by interactions between rudders, and he also found that this critical distance should be less than 1.0 times the chord length of the rudder in order to decrease the turbulence flow and vortices. This result was similar to the findings of Chen et al. (2018), who used numerical simulation to confirming the excellent characteristics of twin-rudder ships compared to single-rudder ships. Chen et al. (2018) concluded that a ship fitted with a twin-rudder configuration would operate very well at 15° rudder angles. Additionally, the twin rudders' effective performance stopped at a lateral spacing equal to 1.3 times the chord length of the rudder.

These previous studies have shown that a rudder system's configuration is the most crucial feature in achieving ship controllability goals. A rudder system must alter ship control to the desired heading angle, due to both internal and external disturbance parameters. The current paper focuses on applying the twin-rudder system to improve ferries' course-keeping quality under windy conditions. By simulating fluctuating wind velocity and directions according to a ship's operating route, quality course-keeping and accurate heading angles may be achieved, increasing the ship's safety.

2. Methods

2.1. Mathematical Model

This study's ship maneuvering analysis used computer simulation to employ modular mathematical models, including a consideration of hydrodynamic derivatives. This study's models were based on surge, sway, and yaw motions (Equation 1) using the coordinate system shown in Figure 1.
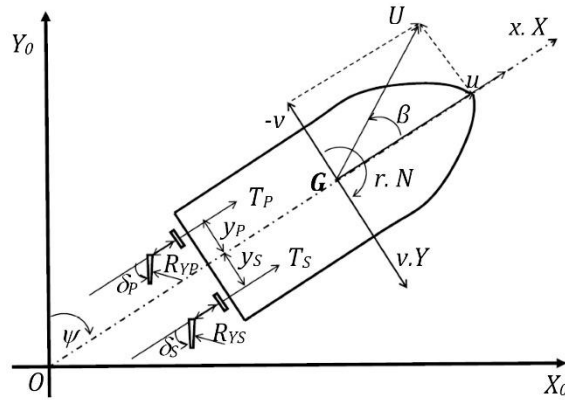

Figure 1 Coordinate ship system

$$m(\dot{u} - rv) = X_H + X_P + X_R + X_W$$
$$m(\dot{v} - ru) = Y_H + Y_P + Y_R + Y_W \tag{1}$$
$$I_{ZZ}\dot{\psi} = N_H + N_P + N_R + N_W$$

The notations u, v and r, are velocity components at the ship's center of gravity (G). m and I_{ZZ} represent the ship's mass and moments of inertia. X, Y, and N represent the hydrodynamic forces and moment. The subscript H, P, R, and W refer to the ship's hull, propeller, rudder, and wind. In principle, the force and moment induced by hull (X_H, Y_H, and N_H) approximate β and r' polynomial function. These equations were expressed by Yoshimura (2001) as Equation 2:

$$X_H = \tfrac{1}{2}\rho L dU^2 (X'_0 + X'_{\beta\beta}\beta^2 + (X'_{\beta r} - m'_y)\beta r' + X'_{rr}r'^2 + X'_{\beta\beta\beta\beta}\beta^4)$$
$$Y_H = \tfrac{1}{2}\rho L dU^2 (Y'_\beta\beta + (Y'_r - m'_x)r' + Y'_{\beta\beta\beta}\beta^3 + Y'_{\beta\beta r}\beta^2 r' + Y'_{\beta rr}\beta r'^2 + Y'_{rrr}r'^3) \tag{2}$$
$$N_H = \tfrac{1}{2}\rho L^2 dU^2 (N'_\beta\beta + N'_r r' + N'_{\beta\beta\beta}\beta^3 + N'_{\beta\beta r}\beta^2 r' + N'_{\beta rr}\beta r'^2 + N'_{rrr}r'^3)$$

where β is the drift angle at the midship position by $\tan^{-1}(v/u)$ and r' non-dimensionalized yaw rate by rL/U. X'_0, $X'_{\beta\beta}$, $X'_{\beta r}$, X'_{rr}, $X'_{\beta\beta\beta\beta}$, Y'_β, Y'_r, $Y'_{\beta\beta\beta}$, $Y'_{\beta\beta r}$, $Y'_{\beta rr}$, Y'_{rrr}, N'_β, N'_r, $N'_{\beta\beta\beta}$, $N'_{\beta\beta r}$, $N'_{\beta rr}$ and N'_{rrr} is the hydrodynamic derivatives on the ship's maneuvering. The force and moment induced by twin-propeller configurations (X_P, Y_P, and N_P) were expressed by Khanfir et al. (2011) in Equation 3:

$$X_P = \rho\left((1 - t_{P(S)})n_{P(S)}^2 D_{P(S)}^4 K_{T(S)}(J_{P(S)}) + (1 - t_{P(P)})n_{P(P)}^2 D_{P(P)}^4 K_{T(P)}(J_{P(P)})\right)$$
$$N_P = \rho\left((1 - t_{P(S)})y_{P(S)}n_{P(S)}^2 D_{P(S)}^4 K_{T(S)}(J_{P(S)}) + (1 - t_{P(P)})y_{P(P)}n_{P(P)}^2 D_{P(P)}^4 K_{T(P)}(J_{P(P)})\right) \tag{3}$$

where $K_{T(S)\atop(P)}(J_{P(S)\atop(P)}) = k_0 + k_1 J_{P(S)\atop(P)} + k_2 J_{P(S)\atop(P)}^2$ and $J_{P(S)\atop(P)} = (u - y_{P(S)\atop(P)}r(1 - w_{P(S)\atop(P)}))/(n_{P(S)\atop(P)}D_{P(S)\atop(P)})$

where t_P is the thrust deduction coefficient in straightforward moving, K_T is the thrust coefficient of the propeller force, and n_P is the propeller revolution. D_P is the propeller diameter, w_P is the effective wake fraction coefficient at the propeller's location, and J_P is

the advance coefficient, while k_0, k_1, and k_2 are the constants for an open-water propeller. The sub-subscript (S) and (P) refer to starboard and portside.

Force and moment due to twin-rudder configurations (X_R, Y_R, and N_R) can be expressed by Equations 4–8 (Khanfir et al., 2011).

$$X_R = -(1-t_{R(S)})F_{RY(S)}\sin\delta_{(S)} - (1-t_{R(P)})F_{RY(P)}\sin\delta_{(P)}$$
$$Y_R = -(1+a_H)\left(F_{RY(S)}\cos\delta_{(S)} + F_{R(YS)}\cos\delta_{(P)}\right)$$
$$N_R = -(x_R + a_H x_H)\left(F_{RY(S)}\cos\delta_{(S)} + F_{RY(P)}\cos\delta_{(P)}\right) + f(x_R)$$
$$f(x_R) = y_{P(S)}(1-t_{R(S)})F_{RY(S)}\sin\delta_{(S)} + y_{P(P)}(1-t_{R(P)})F_{RY(P)}\sin\delta_{(P)}$$

(4)

where δ is the rudder angle, x_R is the rudder's location, and t_R, a_H, and x_H are the interactive force coefficients for the hull, propeller, and rudder as functions of the propeller's advance constant. The rudder's normal (F_{RY}) acting on the rudder stock can be expressed by Equation 5:

$$F_{RY(S)\atop (P)} = \tfrac{1}{2}\rho A_R U_{R(S)\atop (P)}^{2} f_\alpha \sin\alpha_{R(S)\atop (P)}$$

(5)

where A_R is the rudder area, and f_α is the gradient of the rudder's lift coefficient, which can be approximated by the function of the rudder's aspect ratio ($f_\alpha = 6.13\Lambda/(2.25)$). The effective inflow velocity to the rudder (U_R) and the effective angle of attack of the inflow velocity to the rudder (α_R) can be expressed by Equation 6:

$$U_{R(S)\atop (P)} = \sqrt{u_{R(S)\atop (P)}^{2} + v_{R(S)\atop (P)}^{2}} \quad \text{and} \quad \alpha_{R(S)\atop (P)} = \delta_{(S)\atop (P)} - \delta_{R(S)\atop (P)}\left(\beta_{R(S)\atop (P)}\right)$$

(6)

The effective inflow velocity (u_R) to the rudder in the surge direction can be expressed by Equation 7:

$$u_{R(S)\atop (P)} = \varepsilon_{(S)\atop (P)} u_{P(S)\atop (P)} \times \sqrt{\eta_{P(S)\atop (P)}\left\{1 + \kappa\left(\sqrt{1 + 8K_{T(S)\atop (P)}\big/\pi J_{P(S)\atop (P)}^{2}} - 1\right)\right\}^{2} + (1 - \eta_{P(S)\atop (P)})}$$

(7)

where: $\varepsilon_{(S)\atop (P)} = 1 - w_{R(S)\atop (P)}\big/1 - w_{P(S)\atop (P)}$; $\kappa = kx\big/\varepsilon_{(S)\atop (P)}$; $\eta_{P(S)\atop (P)} = D_{P(S)\atop (P)}\big/H_{R(S)\atop (P)}$; $u_{P(S)\atop (P)} = \left(1 - w_{P(S)\atop (P)}\right)\left(u - y_{P(S)\atop (P)}r\right)$

Here, ε, κ, γ_R, and l_R are the parameters describing the rudder inflow velocity angle, while $(1-w_R)$ and η are the propeller wake fraction and effective efficiency, respectively. (D_P/H_R) is the ratio of the propeller diameter to the rudder height.

The effective inflow velocity (v_R) to the rudder in the sway direction can be expressed by Equation 8:

$$v_{R(S)\atop (P)} = u_{R(S)\atop (P)}\tan\left(\delta_{R(S)\atop (P)}\right)$$

(8)

where: $\delta_{R(S)\atop (P)} = \gamma_{R(S)\atop (P)}\beta_{R(S)\atop (P)} + \tan^{-1}\left(y_{R(S)\atop (P)}\big/x_{R(S)\atop (P)}\right)$ and $\beta_{R(S)\atop (P)} = \beta - L_{R(S)\atop (P)}r$

Here, δ_R is the rudder angle, β_R is the effective drift angle at the rudder, and L_R is the flow-straightening coefficient of the yaw rate. For the case of a ship operating under windy conditions, the force and moment (X_W, Y_W, and N_W) acting on the ship were expressed by Equation 9 (Fujiwara and Ueno, 2006):

$$X_W = C_{AX}(\psi_A)q_A A_F; \quad Y_W = C_{AY}(\psi_A)q_A A_L; \quad N_W = C_{AN}(\psi_A)q_A A_L L_{OA} \tag{9}$$

where $\psi_A = \tan^{-1}[U_T\cos\psi + U\cos\beta / U_T\sin\psi - U\cos\beta]$ and $q_A = q_T + q_S + 2\sqrt{q_T q_S}\cos(\psi+\beta)$

C_{AX}, C_{AY}, and C_{AN} are the wind load forces and moments' coefficients, respectively, as a function of the wind direction relative to a ship (ψ_A). U_T and ψ are wind velocity and direction angles with reference to the coordinate system, q_A is wind pressure, q_T is wind pressure due to the elevation of the center of a windage area, and q_S is the wind pressure induced by wind velocity, without an elevation effect. A_F and A_L are the transversal and lateral projections of the windage area, respectively.

2.2. Autopilot Ship Steering

The rudder is the most critical feature in achieving controllability goals (Lee et al., 2009). The control system must alter the control surfaces to the desired heading angle. The schematic equation of the PID control system that a ship tracks can be expressed by Equation 10 (Lee et al., 2009).

$$\delta = K_P(e) + K_d(\dot{e}) + K_i \int_0^T e(t)dt \text{ and } e = (\psi_T - \psi_P) \tag{10}$$

where δ is designed rudder angle; K_p, K_d, and K_i are proportional gain, derivative gain, and integral gain respectively; and e is an error between the heading target (ψ_T) and the actual heading angle (ψ_P). Furthermore, the line-of-sight (LOS) method (Fossen, 2002) helps control ships reach target headings through reference heading angles. The reference heading angle equation and target zone correction can be expressed by Equation 11:

$$\psi_{ref}(t) = \tan^{-1}(y_k - y(t)/x_k - x(t)) \text{ and } (x_k - x(t))^2 + (y_k - y(t))^2 \leq R_0^2 \tag{11}$$

where x_k and y_k are the track-point coordinates, $x(t)$ and $y(t)$ are the ship's coordinates position, and R_0 is the target zone's radius.

2.3. Simulation Program

According to IMO (2002) criteria for ship maneuvering, a swept path should be used to analyze a ship's course-keeping prediction. A ship's swept path can be obtained by double-integrating the ship motion mathematical model's acceleration, including hydrodynamic derivatives. A numerical integration of the Dormand–Prince method (Maimun et al., 2013; Muhammad et al., 2015) then solved the equations of motion in this time-domain simulation using the MATLAB-Simulink program. The coefficient of hydrodynamic derivatives for the acting hull force and moment in Equation 2—and the interaction force coefficient among the hull, propeller, and rudder—were predicted using the derived regression equation developed by Yoshimura and Masumoto (2012). This regression equation is among the models used by Sukas et al. (2019) in developing the SINMAN Program to predict turning circles and zigzag maneuvering for ships with twin-rudder and twin-propeller systems, as well as validation through model testing or free-running tests. In many cases, the regression equation has been used to predict ferry ships' maneuvering under active wind and wave conditions (Paroka et al., 2015, 2016, 2017b). A ship's resistance coefficients for simulation were predicted using the Holtrop method (Holtrop and Mennen, 1982; Holtrop, 1984). The propeller thrust coefficient ($K_T(J_P) = 0.4061 - 0.3034 J_P - 0.1178 J_P{}^2$) was predicted using polynomial regression, based on the open water test's statistical data for the B-series propeller (Carlton, 2007). The coefficient of the wind load force and moment in Equation 9 was predicted using the methodology proposed by Fujiwara and Ueno (2006). The control method used in the simulation was a proportional integrated derivative (PID) controller. The designed rudder angle ($\delta=\pm35$ deg.) was

calculated using Equation 10 with a PID gain (K_p = 2.208; K_i = 0.027 and K_d = 45.372), and it was selected using the pole placement method with the second-order linear Nomoto model of the ship (Nomoto et al., 1957). The methods used by Paroka et al. (2017a) in developing an automatic control system to predict and avoid ferry-ship collisions were compared using a free-running experiment.

2.4. Ship and Sea-Trial Data

The study's object was the *KMP Bontoharu* ferry ship (1053 gross tonnage), owned by PT. ASDP Indonesia Ferry. The ship has twin propellers and twin rudders, and the distance between the rudders and propellers is 2.3 m. The ship's particulars are presented in Table 1. The ship's sea trial on the Selayar-to-Bulukumba route was 15.385 nautical miles long, involving a 7,268-second traveling time, around a 6.03 m/s wind velocity, and a 254° wind direction. The trial data were taken on September 20, 2015.

Table 1 Ship particulars

Hull	Value	Super structure	Value	Propeller and rudder	Value
Loa, m	54.00	A_L, m^2	182.87	*Z*	2×4
Lbp,m	47.45	A_F, m^2	129.20	*D, m*	1.450
B, m	14	A_{OD}, m	218.23	*Ae/Ao*	0.645
H, m	3.4	*C*	-0.44	*Pitch, m*	1.320
T,m	2.45	H_C, m	2.70	*n*	8.784
$V, m/s^2$	6.618	H_L, m	3.38	*Span, m*	1.550
Δ, Ton	1148	H_{BR}, m	10.48	*Chord, m*	0.900
				A_R, m^2	2×1.395
				BHP, HP	2×1000
				RPMME	1850

2.5. Wind Data

Monthly wind velocity data were obtained from ERA-Interim reanalysis data from the European Centre for Medium-Range Weather Forecasts (ECMWF) for 10 years, from 2006 to 2018, at six-hour intervals. The model provided wind speed data with a resolution of 0.25 × 0.25 degrees. This model was validated by Dee et al. (2011). Furthermore, it was validated locally by Lina et al. (2015) using data from eight buoys deployed in the Yellow Sea and the East China Sea. This study's coordinate for its observation data was at 5.75°S and 120.5°E.

3.   Results and Discussion

The wind speed trend peaked in January, with a maximum of 10.06 m/s (88°), as Figure 2 shows. Meanwhile, April's monthly wind speed trend decreased, with a minimum of 6.41 m/s (219°). The monthly wind speed movements varied, depending on the month occurring during the west or east monsoon seasons.
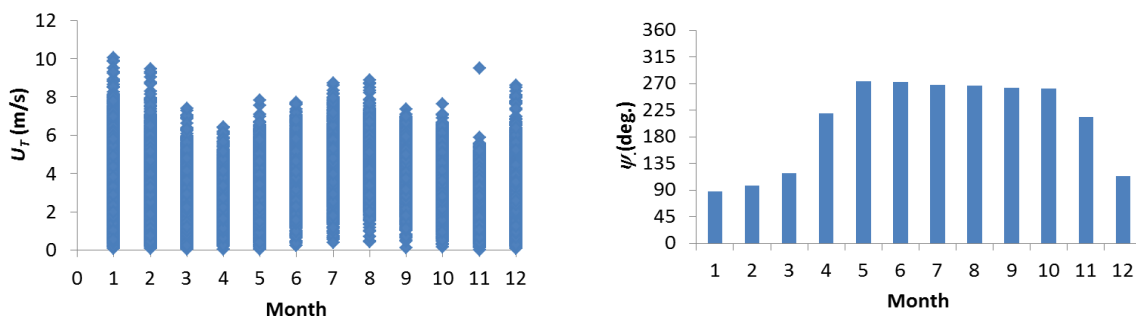

Figure 2 Significant wind velocity and direction on the Selayar–Bulukumba route

Based on the wind data characteristics in Figure 2, the *KMP Bontoharu*'s course-keeping was simulated for three conditions of wind direction parameters—the starboard bow (88°) and the portside stern of the ship (219° and 268°)—using the time domain simulation program of MATLAB-Simulink. This information is essential to ship navigation due to time-savings and reduced fuel consumption by controlling a twin-rudder configuration design. Figure 3 shows the historic result of the simulation for the course-keeping trajectory of the *KMP Bontoharu* (Selayar to Bulukumba) under wind velocities' effect.
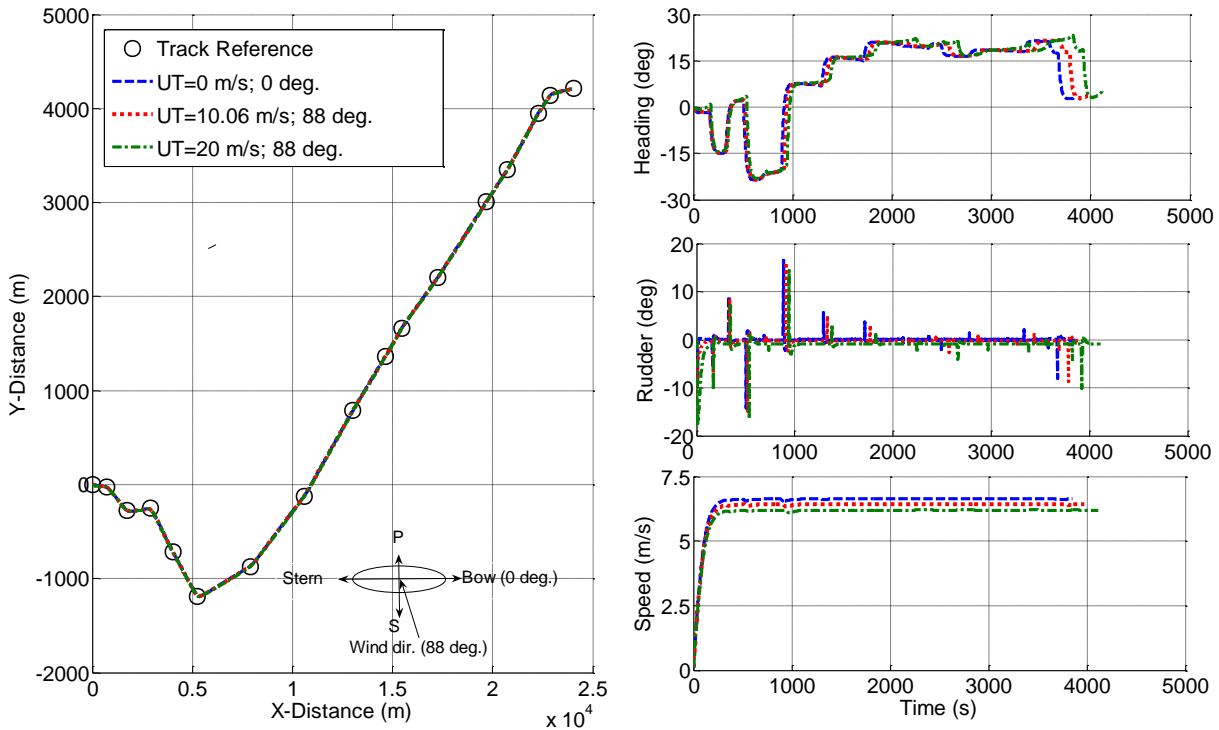
Figure 3 Ship trajectory with different wind speeds (U_T) at 88°

The horizontal axis expresses the time, while the vertical axis expresses the heading angle (ψ), rudder angle (δ), and ship speed (u), respectively. The wind blew from the starboard bow (88°) at wind velocities of 10.06 m/s for the initial ship speed (U) of 6.618 m/s. We found that the course-keeping trajectory slowly deviated from the initial track with a low heading with significant course-keeping time compared to conditions without winds (U_T = 0 m/s). Meanwhile, the ship's course-keeping trajectory with increased wind velocities caused more deviations and low ship speeds.
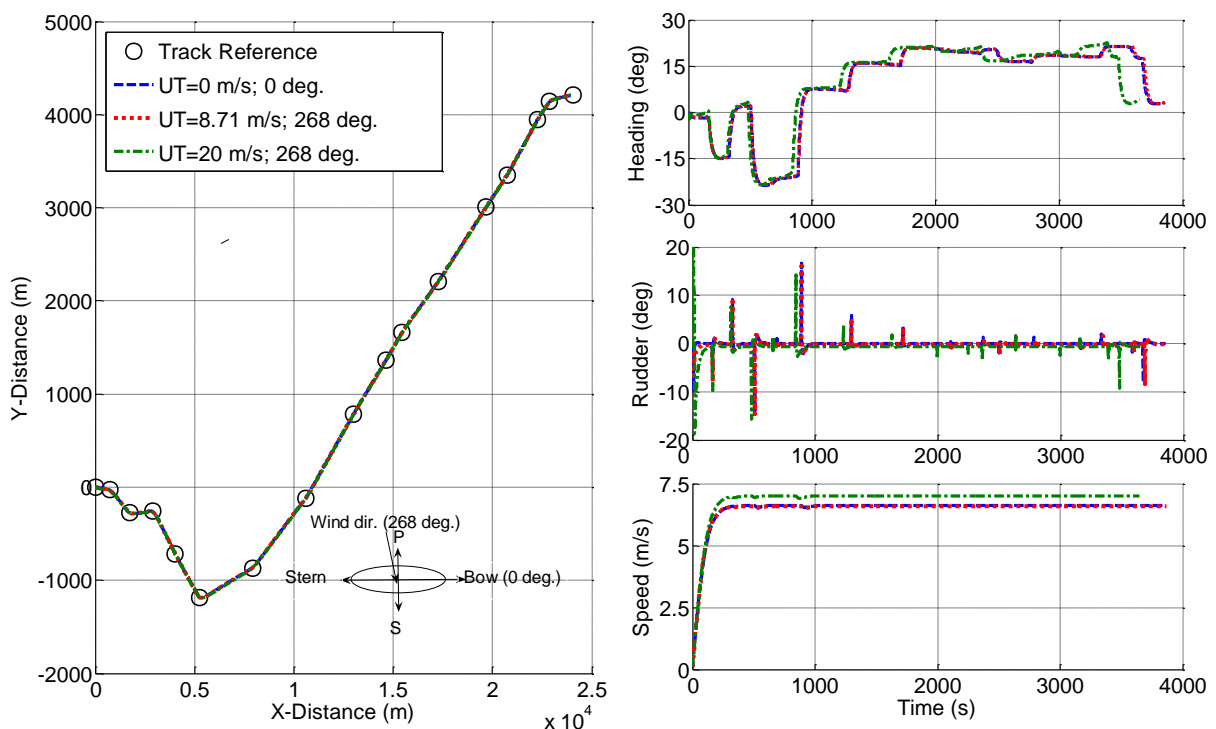
Figure 4 shows the simulation results for the *KMP Bontoharu*'s course-keeping with the wind blowing from the portside stern (219°) at a wind velocity range of 0–20 m/s for the initial ship speed (U) of 6.618 m/s. We found that the course-keeping trajectory quickly deviated from the initial track with a high heading and short course-keeping time at each blown wind velocity, compared to conditions without winds (U_T = 0 m/s). These characteristics differed when the wind blew from the starboard side (88°). The wind direction angle caused these differences, as Ohtsu et al. (1996) found, relating to changes in a ship's heading and rudder angle as a result of wind velocity and ship direction in course-keeping.
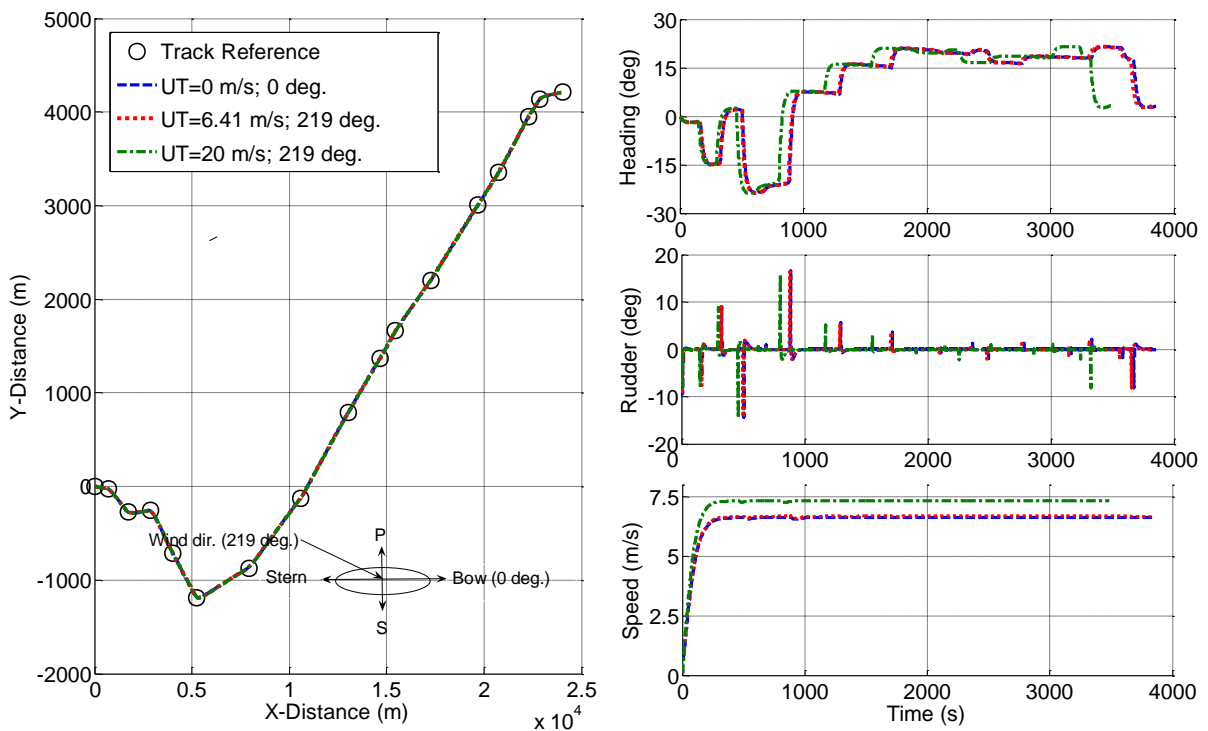
Figure 4 Ship trajectory with different wind speeds (U_T) at 219°

Figure 5 shows the historic results of the simulation for the course-keeping trajectory of the *KMP Bontoharu* with the wind blowing from the portside stern (268°) at a wind velocity range of 0–20 m/s for the initial ship speed (U) of 6.618 m/s. At a wind velocity of 8.71 m/s, the ship's speed was 0.27% reduced compared to conditions without wind (U_T = 0 m/s), while the ship speed increased by 5.96% increases at a wind speed of 20 m/s. These changes in ship speed were caused by the ship's directional movements.

Figure 5 Ship trajectory with different wind speeds (U_T) at 268°

Figure 6 shows the sea-trial simulation results for the ship course-keeping trajectory with a 6.03 m/s wind velocity and a 254° wind direction at an initial ship speed of 3.98 m/s. We found that the traveling time under these conditions stood at 6,407 seconds. The simulation's traveling time was 11.84% higher than the sea-trial result. A possible reason for this difference is that the simulation excluded waves and currents.
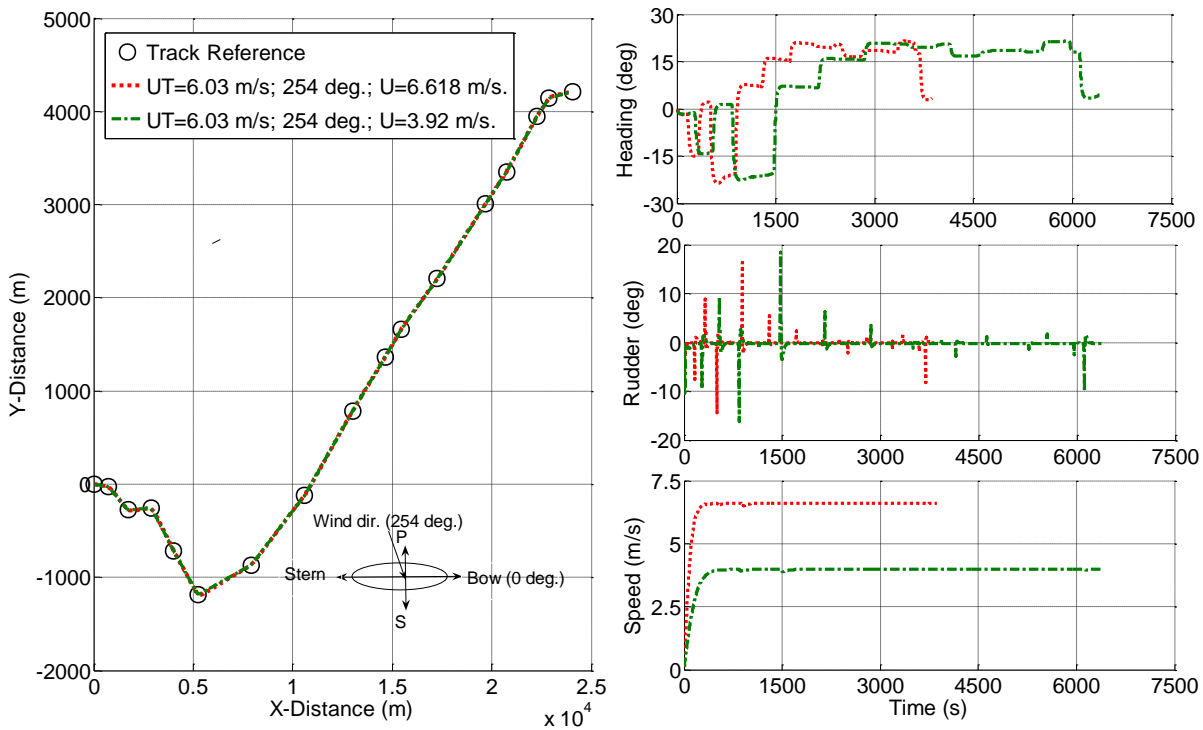

Figure 6 Sea-trial simulation result for ship trajectories with different initial ship speeds (U)

Figures 3, 4, and 5 also show the effects of winds velocity and direction on ship speed, with a course-keeping trajectory for an initial ship speed (U) of 6.618 m/s. We found that, when the wind blew from the starboard bow (88°) with a wind velocity of 20 m/s, the ship speed was 6.36% lower compared to conditions without wind ($U_T = 0$ m/s). Meanwhile, when the wind blew from the portside stern (219° and 268°), the ship speed was increased by 10.74% and 5.96%, respectively. The two latter speeds were beneficial because the track trajectory times were minimal.
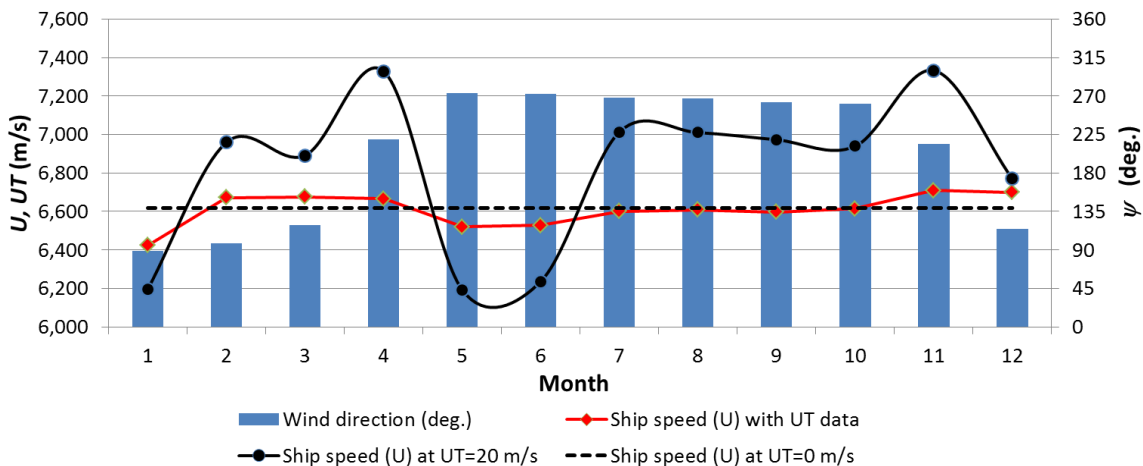

Figure 7 Tracking ship speed trajectories with different wind velocities and directions

In general, when the wind blew from the starboard and portside to the stern (98° to 268°), the ship's track trajectory time tended to benefit compared to conditions with the wind blows from the bow to the starboard and portside, as the simulation results in Figure 7. The ship's reduced speed when the wind blew from the bow to the starboard (less than 100°) was similar to the findings of Paroka et al. (2016) related to ship-speed changes caused by wind speeds and directions' influence on ferry maneuvering.

4. Conclusions

This study has analyzed a twin-rudder-system configuration's influence on a ship's course-keeping ability under various wind speeds and directions through the MATLAB-Simulink computer-simulation program. The results indicated that applying a twin-rudder system to ferry ships' to improve their course-keeping ability under windy conditions is very effective using a PID controller, reducing ship deviation and increasing ship speed by adjusting the ship's heading angle to the desired path. The track trajectory time in the ferry's course-keeping highly depends on wind velocity and direction. When the wind blows from the starboard and portside to the stern (98 to 268°), a ship's travel time tends to benefit compared to when the wind blows from the bow to the side. This research shows that the PID controller method can be applied to assist ships' movements due to other environmental influences, such as waves and currents. However, ships' course-keeping quality highly depends on the selected PID parameters.

Acknowledgements

References

Carlton, J., 2007. *Marine Propellers and Propulsions.* Second edition. London, Elsevier Ltd.

Chen, L., Zhu, X., Zhou, L., 2018. Hydrodynamic Characteristics of Twin Rudders. *In:* Proceedings of International Conference on Computational Methods, Volume 5, pp. 638–649

Dee, D.P., Uppala, S.M., Simmons, A.J., Berrisford, P., Poli, P., Kobayashi, S., Andrae, U., Balmaseda, M.A., Balsamo, G., Bauer, P., Bechtold, P., Beljaars, A.C.M., van de Berg, L., Bidlot, J., Bormann, N., Delsol, C., Dragani, R., Fuentes, M., Geer, A.J., Haimberger, L., Healy, S.B., Hersbach, H., Holm, E.V., Isaksen, L., Kallberg, P., Kohler, M., Matricardi, M., NcNally, A.P., Monge-Sanz, B.M., Morcrette, J.-J., Park, B.-K., Peubey, C., de Rosnay, P., Tavolato, C., Thepaut, J.-N., Vitart, F., 2011. The ERA-Interim Reanalysis: Configuration and Performance of the Data Assimilation System. *Quarterly Journal of the Royal Meteorological Society*, Volume 137, pp. 553–597

Fossen, T.I., 2002. *Marine Control Systems: Guidance, Navigation and Control of Ships, Rigs and Underwater Vehicles*. Trondheim, Norway, Marine Cybernetics AS

Fujiwara, T., Ueno, M., 2006. Cruising Performance of a Large Passenger Ship in Heavy Sea. *Proceedings of the Sixteenth International Conference on Offshore and Polar Engineering*, Volume 3, pp. 304–311

Gim, O.S., 2013. Assessment of Flow Characteristics A Round Twin Rudder with Various Gaps Using PIV Analysis in Uniform Flow. *Ocean Engineering*, Volume 66, pp. 1–11

Hasegawa, K., Kang, D., Sano, M., Nagarajan, V., Yamaguchi, M., 2006. A Study on Improving the Course-Keeping Ability of a Pure Car Carrier in Windy Conditions. *Journal of Marine Science and Technology*, Volume 11(2), pp. 76–87

Holtrop, J., Mennen, G.G.J., 1982. An Approximate Power Prediction Method. *Journal of International Shipbuilding Progress*, Volume 29, pp. 166–170

Holtrop, J., 1984. A Statistical Re-Analysis of Resistance and Propulsion Data. *Journal of International Shipbuilding Progress*, Volume 31, pp. 272–276

IMO, 2002. Standards for Ship Maneuverability. Report of the Maritime Safety Committee on Its Seventy-Sixth Session-Annex 6 (Resolution MSC. 137(76)). London UK

Khanfir, S., Hasegawa, K., Lee, S.K., Jang, T.S., Lee, J.H., Cheon, S.J., 2008. 2008K-G4-3 Mathematical Model for Maneuverability and Estimation of Hydrodynamic Coefficients of Twin-Propeller Twin-Rudder Ship. *In:* Proceedings of the Japan Society of Naval Architects and Ocean, Volume 6, pp. 57–60

Khanfir, S., Hasegawa, K., Nagarajan, V., Shouji, K., Lee, S.K., 2011. Manoeuvring Characteristics of Twin-Rudder Systems: Rudder-Hull Interaction Effect on the Manoeuvrability of Twin-Rudder Ships. *Journal of Marine Science and Technology*, Volume 16, pp. 472–490

Lee, G., Surendran, S., Kim, S.H., 2009. Algorithms to Control the Moving Ship During Harbour Entry. *Applied Mathematical Modelling*, Volume 33(5), pp. 2474–2490

Lina, S., Zhiliang, L., Fan, W., 2015. Comparison of Wind Data from ERA-Interim and Buoys in the Yellow and East China Seas. *Chinese Journal of Oceanology and Limnology*, Volume 33(1), pp. 282–288

Maimun, A., Priyanto, A., Rahimuddin, Sian, A.Y., Awal, Z.I., Celement, C.S., Nurcholis, Waqiyuddin, M., 2013. A Mathematical Model on Manoeuvrability of a LNG Tanker in Vicinity of Bank in Restricted Water. *International Journal of Safety Science*, Volume 53, pp. 34–44

Muhammad, A.H., Hasbullah, M., Djabbar. M.A., Handayani, H., 2015. Comparison Between Conventional and Azimuthing Podded Propulsion on Maneuvering of a Ferry Utilizing Matlab Simulink Program. *International Journal of Technology*, Volume 6(3), pp. 452–461

Nomoto, K., Taguchi, T., Honda, K., Hirano, S., 1957. On the Steering Qualities of Ships. *International Shipbuilding Progress*, Volume 4(35), pp. 354–370

Ohtsu, K., Shoji, K., Okazaki, T., 1996. Minimum-Time Maneuvering of a Ship, with Wind Disturbances. *IFAC Proceedings Volumes*, Volume 28(2), pp. 338–345

Paroka, D., Muhammad, A.H., Asri, S., 2015. Steady State Equilibrium of Ships Maneuvering under Combined Action of Wind and Wave. *Jurnal Teknologi (Science and Engineering),* Volume 76(1), pp. 67-75.

Paroka, D., Muhammad, A.H., Asri, S,. 2016. Maneuverability of Ships with Small Draught in Steady Wind. *Makara Journal of Technology*, Volume 20(1), pp. 24-30

Paroka, D., Kamil. M.F, Muhammad, A.H., 2017a. Experimental Study on Automatic Control for Collision Avoidance of Ships. *Makara Journal of Technology*, Volume 21(3), pp. 137–144

Paroka, D., Muhammad, A.H., Asri, S., 2017b. Prediction of Ship Turning Maneuvers in Constant Wind and Regular Wave. *International Journal of Technology*, Volume 8(3), pp. 387–397

Paroka, D., 2020. Yaw Motion Stability of an Indonesian Ro-Ro Ferry in Adverse Weather Conditions. *International Journal of Technology*, Volume 11(4), pp. 862–872

Prpic-Orsic, J., Vettor, R., Faltinsen, O.M., Soares, C.S., 2016. The Influence of Route Choice and Operating Conditions on Fuel Consumption and CO_2 Emission of Ships. *Journal of Marine Science and Technology*, Volume 21(3), pp. 434–457

Sukas, O.F., Kinaci, O.K., Bal, S., 2019. Theoretical Background and Application of MANSIM for Ship Maneuvering Simulations. *Ocean Engineering,* Volume 192, pp. 1–20

Yoshimura, Y., 2001. Investigation into the Yaw-Checking Ability in Ship Maneuverability Standard. *In:* Proceeding of Prediction of Ship Maneuvering Performance. Tokyo, Japan. pp. 11–19

Yoshimura, Y., Sakurai, H., 1989. Mathematical Model for the Manoeuvring Ship Motion in Shallow Water (3rd Report). *Journal of Kansai Society of Naval Architects*, Volume 211, pp. 115–126

Yoshimura, Y., Masumoto, Y., 2012. Hydrodynamic Database and Manoeuvring Prediction Method with Medium High-Speed Merchant Ships and Fishing Vessels. *Proceeding International Conference on Marine Simulation and Ship Manoeuvrability 2012*, Singapore, *International Marine Simulation Forum*. pp. 494–503